Acta Crystallographica Section B
Structural Science
ISSN 0108-7681

Two phases of $C_9H_{12}O_4$: why is the structure at 295 K so complicated?

Laura L. Duncan, Brian O. Patrick and Carolyn Pratt Brock*

Department of Chemistry, University of Kentucky, Lexington, KY 40506-0055, USA

Correspondence e-mail: cpbrock@uky.edu

Received 6 September 2001
Accepted 10 January 2002

Molecules of 4,4′-dimethyl-2-hydroxy-6-oxocyclohexene-1-carboxylic acid, $C_9H_{12}O_4$, crystallize at 295 K in a modulated superstructure with five half-molecules in the asymmetric unit; each molecule is located on one of the mirror planes of the space group $Cmc2_1$. Reflections with $k \neq 5n$ are systematically weak; a satisfactory refinement can be obtained in a *Cmcm* pseudocell having $\mathbf{b}' = \mathbf{b}/5$. The important modulation involves small rotations of the molecules around axes perpendicular to the mirror plane; there is also an up/down disorder of the CMe_2 fragment in four of the five molecules (two molecules with occupancy factors *ca* 4:1; two with occupancy factors *ca* 3:2). The modulation is a response to packing problems that can be traced to the differences between the thin, electron- and oxygen-rich 'head' of the molecule and the thicker, methyl-rich 'tail'. At 130 K the length of **b** is reduced by 2/5 and the *Pmnb* structure is ordered. Both structures can be described as modulated variants of the *Cmcm* substructure; the wavevectors are $2\mathbf{b}'^*/5$ for the room-temperature structure and $\mathbf{b}'^*/2$ for the low-temperature structure, where $\mathbf{b}'^*$ is the reciprocal axis of the subcell. The structure at room temperature can also be understood as a hybrid of the fully disordered pseudocell structure and the ordered structure that is found at low temperature.

1. Introduction

The structure of 4,4′-dimethyl-2-hydroxy-6-oxocyclohexene-1-carboxylic acid (hereafter, ME2C7O4) was undertaken to see if any difference between the C2 (C—OH) and

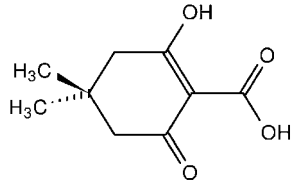

C6 (C═O) positions could be detected. That hope was not realised,[1] but the structure at room temperature proved interesting because Z' (the number of molecules in the asymmetric unit) is exceptionally large (Brock & Dunitz, 1994). The structure at 295 K (hereafter, RT) is a modulated

[1] A detailed study at 19 K (Roversi *et al.*, 1996) of the electron density in the citrinin molecule, a fungal metabolite that also contains the C(OH)C(COOH)C(═O) fragment, appeared after this work was begun. The OH protons in citrinin are ordered at 147 K and below (Destro & Marsh, 1984) and all hydrogen bonding is intramolecular. At 19 K the measured differences between the C—OH and C═O bond lengths are 0.07 Å for the carboxylic acid group and 0.05 Å for the ring substituents.

Table 1
Experimental details.

	RT	LT
Crystal data		
Chemical formula	$C_9H_{12}O_4$	$C_9H_{12}O_4$
Chemical formula weight	184.19	184.19
Cell setting, space group	Orthorhombic, $Cmc2_1$	Orthorhombic, $Pmnb$
a, b, c (Å)	10.474 (5), 66.24 (3), 6.662 (3)	10.471 (3), 26.240 (9), 6.434 (2)
V (Å^3)	4622 (4)	1767.8 (10)
Z	20	8
Imposed symmetry	m	m
D_x (Mg m^{-3})	1.323	1.384
Radiation type	Mo $K\alpha$	Mo $K\alpha$
No. of reflections for cell parameters	23 801	23
θ range (°)	1.0–27.5	8.6–15.7
μ (mm^{-1})	0.104	0.109
Temperature (K)	295 (1)	130 (2)
Crystal form, colour	Laths, colourless	Laths, colourless
Bounding planes	{150}; {010}	{120}; {010}
Crystal size (mm)	0.50 × 0.30 × 0.15	0.38 × 0.35 × 0.10
Data collection		
Diffractometer	Nonius Kappa–CCD	Nonius CAD-4
Data collection method	φ and ω scans with 2.0° steps	ω scans
No. of measured, independent and observed parameters	11 377, 2987, 1388	960, 465, 250
Criterion for observed reflections	$I > 2\sigma(I)$	$I > 2\sigma(I)$
Symmetry for averaging	mmm	mmm
R_{int}	0.048	0.131
θ_{max} (°)	27.5	16.0
Range of h, k, l	$0 \rightarrow h \rightarrow 13$ $0 \rightarrow k \rightarrow 85$ $-8 \rightarrow l \rightarrow 8$	$0 \rightarrow h \rightarrow 8$ $0 \rightarrow k \rightarrow 20$ $-4 \rightarrow l \rightarrow 4$
No. and frequency of standard reflections	–	2 every 60 min
Refinement		
Refinement on	F^2	F^2
$R[F^2 > 2\sigma(F^2)]$, $wR(F^2)$, S	0.070, 0.191, 1.5	0.081, 0.214, 1.43
No. of reflections and parameters used in refinement	2987, 388	465, 20
No. of restraints	430	8
H-atom treatment	Constrained	Constrained
Weighting scheme	$w = 1/[\sigma^2(F_o^2) + (0.06P)^2]$, where $P = (F_o^2 + 2F_c^2)/3$	$w=1/[\sigma^2(F_o^2) + (0.06P)^2]$, where $P = (F_o^2 + 2F_c^2)/3$
$(\Delta/\sigma)_{max}$	0.001	0.001
$\Delta\rho_{max}$, $\Delta\rho_{min}$ (e Å^{-3})	0.17, −0.15	0.42, −0.35

Computer programs used: *COLLECT* (Enraf–Nonius, 1988), *DENZO-SMN*, *SCALEPACK* (Otwinowski & Minor, 1997), *SHELXL*97 (Sheldrick, 1997), *SHELXTL/PC* (Sheldrick, 1990).

superstructure with five half-molecules in the asymmetric unit. Solution, refinement and interpretation of the structure was complicated further by an up/down disorder of the CMe_2 part of four of the five molecules. The structure at 130 K (hereafter, LT) has a smaller unit cell [$\mathbf{b}_{LT} = (2/5)\,\mathbf{b}_{RT}$] that is ordered, but there are still two independent half-molecules, which are related by pseudosymmetry. In both structures the molecules lie on crystallographic mirror planes that pass through the Me_2C unit and that make the two sets of oxo and hydroxyl O atoms equivalent. Both structures can be understood as modulated forms of a fully disordered *Cmcm* pseudocell structure.

The transition between the RT and LT phases involves two types of structural change. The first is the ordering of the CMe_2 fragments; the second is the tilting of the molecules with respect to the stacking axis **c**, which is approximately perpendicular to the O-atom plane and which lies in the crystallographic mirror plane. This phase behavior is similar to that seen for 1,3-cyclohexanedione, its 2-methyl derivative, and related compounds (Katrusiak, 1992, 2000). The molecules studied by Katrusiak are normally found as the enol tautomers and so are closely related to the molecule described here. The ME2C7O4 system of phases differs from the diones studied previously because the higher-temperature phase is partially ordered and modulated rather than fully disordered and because all hydrogen bonding is intramolecular rather than intermolecular.

2. Experimental

2.1. Synthesis

Treatment of 5,5-dimethylcyclohexane-1,3-dione (0.560 g, 4.0 mmol) with 20 ml of 2 *M* magnesium methyl carbonate (Aldrich) in DMF at 408 K for 1 h, followed by quenching in 100 g ice containing 10 ml HCl, produced a nearly colorless precipitate, which was taken up in ether. The ether solution was washed with water, then with saturated NaCl and dried over Na_2SO_4. Removal of solvent yielded 0.727 g of crude product. Recrystallization at RT from ethyl ether provided 0.555 g (75%) of colorless crystals. ^{1}H NMR (200 MHz, $CDCl_3$): δ 1.139 (s, 6H), 2.527 (s, 4H), 14.811 (s, 2H); λ_{max} (EtOH) 257 (ε 10,300), 220 nm (ε 5,200). The compound melted at 396 K to a clear liquid which immediately evolved gas (presumably CO_2) vigorously. Upon cooling the melt, crystals of pure 5,5-dimethylcyclohexane-1,3-dione (m.p. 421 K) were formed.

Unsubstituted 2-hydroxy-6-oxo-cyclohexene-1-carboxylic acid and its 3,3′-dimethyl derivative were also synthesized by this route, but neither could be coaxed to give crystals that diffracted well.

2.2. Diffraction data

Crystals were first examined at room temperature with a Nonius CAD-4 diffractometer. Diffraction data for crystals

Table 2
Intensity as a function of mod(k,5) [$\sin(\theta/\lambda)_{max}$ = 065 Å^{-1}].

mod(k,5)	No. of unique data	% having $I > 2\sigma(I)$	% having $I > 10\sigma(I)$
0	575	78	55
1, 4	1211	25	5
2, 3	1201	53	28
All	2987	46	24

studied in 1993 and 1994 indicated a C-centered supercell with cell lengths $a = 10.46$, $b = 5 \times 13.23$, $c = 6.65$ Å, and with angles very close to 90°. The first set of data was collected with Mo $K\alpha$ radiation to $\theta = 27.5°$, but only 20% of the unique reflections had $I > 3\sigma(I)$. Furthermore, the intensity standards decreased by 22% during the several days of data collection, even though the crystal was encased in epoxy. These data, however, did allow solution of the pseudocell structure and determination of many of the characteristics of the modulated structure. The second crystal studied gave the same unit cell, but decomposed much more rapidly. Under the microscope it was obvious that this second crystal, which was also coated with epoxy, was reacting. Since the crystals are stable for several months in light and air, we suspect that the X-ray beam initiates a free-radical process that leads to the loss of CO_2 (see §2.1).

In 1997 we attempted data collection at low temperature (130 K), but the crystal was lost after data to $\theta = 16°$ had been measured. There was no indication of significant intensity loss before the crystal disappeared. The strains associated with unit-cell contraction (see below) probably caused the crystal to fracture.

The problem was revisited after installation of a Nonius KappaCCD diffractometer. Three crystals were examined at room temperature; all three gave the $b = 5 \times 13.23$ Å cell seen previously. When the camera distance was set at 60 mm (graphite-monochromated Mo $K\alpha$ radiation; $\lambda = 0.71073$ Å) there was no problem with reflection overlap. An oscillation pattern recorded around the **b** axis showed that the peaks had normal shapes. That pattern has been deposited.[2]

Data were collected with the CCD diffractometer (see Table 1) under the control of the program *COLLECT* (Nonius, 1998); cell dimensions were determined and the data reduced with *DENZO-SMN* (Otwinowski & Minor, 1997). When the PRECESSION routine in *COLLECT* became available (Nonius, 1999) the data in the frames were transformed to show all the scattering in the slices $nk\ell$, $hn\ell$ and hkn, n = 0–3. The superlattice reflections are sparse (see Table 2) for reflections with mod(k,5) = 1 and 4, but reflections with mod(k,5) = 2 and 3 are only somewhat weak. We saw no evidence of any diffuse scattering or of any unusual peak shapes.

Wilson plots for the classes of reflections shown in Table 2 (see Xia *et al.*, 2001) have been deposited. They show that at $\theta = 13°$ the ratios of the average normalized intensities of the $k = 5n \pm m$, m = 0, 1 and 2 reflections are 70: 1: 10. Those ratios are reduced to 8:1:2 at $\theta = 25°$ ($\sin\theta/\lambda = 0.60$ Å^{-1}) because the small differences between pseudosymmetrically related molecules become more important as the scattering angle increases.

The data at 130 K were collected with a CAD-4 serial diffractometer under control of the Enraf–Nonius (1988) software. Data collection for the first shell (to 16° θ) was straightforward, but the crystal disappeared shortly after the second shell was begun.

2.3. Crystal morphology

Crystals from all recrystallization batches looked the same under the microscope; they are laths that are longest in the **c** direction and that have pointed ends. The two largest faces are related by an inversion center and belong to the {150} form of the RT cell (*i.e.* the {110} form of the pseudocell). The other two faces that are parallel to **c** are smaller and less well formed; they did not reflect light well when the crystals were mounted on an optical goniometer. We were never able to assign indices for this second set of faces with confidence. In several crystals the faces seemed to be the other two members of the {110} form of the pseudocell and in other crystals the faces seemed to belong to the form {010}. The crystals were terminated along ±**c** by the two largest faces of the {150} form and by two small faces having $\ell \neq 0$ [*i.e.* $(15\bar{\ell})$ if the largest faces are (150) and $(\bar{1}50)$].

2.4. Structure determinations

Results are presented (see Table 1) for a restrained refinement of the RT structure and for a limited refinement of the LT structure. The output files for the final sets of least-squares cycles are included with the supplementary material.

The values of $wR(F^2)$ and S depend strongly on the weights chosen for the intensities. In the end we chose a very conventional scheme (see Table 1) even though it leads to values of S well above 1.

2.4.1. Room-temperature pseudocell structure. The RT structure was solved without difficulty with *SIR*92 (Altomare *et al.*, 1994) in a C-centered orthorhombic pseudocell having $b = 13.23$ Å after all reflections with $k \neq 5n$ were discarded and the remaining reflections were transformed so that $k' = k/5$ (2371 measured and 575 unique reflections; $R_{int} = 0.031$). Structure solutions were obtained for space groups *Cmcm* and $Cmc2_1$. In both groups the molecule lies on a mirror plane that passes through all three C atoms of the CMe_2 fragment. The group *Cmcm* requires that the molecule lie on an *m*2*m* site, in which case the CMe_2 part of the molecule must be disordered over two orientations. The group $Cmc2_1$ does not require disorder of the CMe_2 group, but disorder was found; the bond to the axial methyl atom points in two directions (occupancy factors 0.6 and 0.4) related by a mirror plane perpendicular to **c**.

The structures were refined on F^2 using *SHELXL*97 (Sheldrick, 1997). The H atoms were treated as in the superstructure (see below). The refinement in $Cmc2_1$ had somewhat

[2] Supplementary data for this paper are available from the IUCr electronic archives (Reference: BR0109). Services for accessing these data are described at the back of the journal.

Table 3
Average bond lengths (Å) and angles (°) for the structure at 295 K (n = 5).

Atom 1	Atom 2	Distance in pseudocell refinement	Average distance in full refinement
O1	C7	1.267 (2)	1.271 (3; 2)
O3	C2	1.267 (2)	1.272 (3; 3)
C1	C7	1.451 (4)	1.458 (5; 2)
C1	C2	1.398(2)	1.404 (4; 1)
C2	C3	1.568 (3)	1.528 (5; 6)
C3	C4	1.542 (3)	1.519 (5; 3)
C4	C8	1.557 (4)	1.525 (6; 3)
C4	C9	1.484 (5)	1.558 (7; 4)

Atom 1	Atom 2	Atom 3	Angle in pseudocell refinement	Angle in full refinement
O1	C7	$O1^m$	120.7 (2)	120.9 (5; 5)
O1	C7	C1	119.6 (1)	119.5 (2; 2)
O3	C2	C1	122.3 (2)	121.6 (3; 1)
O3	C2	C3	115.6 (2)	116.2 (4; 4)
C2	C1	$C2^m$	120.9 (2)	120.1 (4; 1)
C7	C1	C2	119.6 (1)	119.8 (2; 1)
C1	C2	C3	118.2 (2)	118.7 (4; 7)
C2	C3	C4	108.5 (2)	111.9 (4; 7)
C3	C4	$C3^m$	122.4 (2)	109.1 (6; 6)
C3	C4	C8	107.2 (2)	110.3 (4; 5)
C3	C4	C9	112.3 (2)	109.2 (4; 4)
C8	C4	C9	111.2 (3)	108.9 (6; 5)

Numbers in parentheses are the estimated standard uncertainties in the least-significant digits. When two s.u.s are given the first refers to the average s.u. calculated from the individual coordinates and the second is the s.u. of the mean. Atoms in pairs designated *e.g.* O1/$O1^m$ are related by the mirror plane that bisects the molecule.

lower agreement factors (R_1/wR_2 = 0.060/0.178 *versus* 0.063/0.198), but the ratio of observations to parameters (575/85 = 6.8 *versus* 575/52 = 11.1) was abnormally low and convergence was poor. These refinement problems arise because the disordered $Cmc2_1$ structure is nearly centrosymmetric. If the occupancy factor were 0.500 rather than 0.570 (5) and if atoms O1, O3, C1, C2 and C7 (see Fig. 1) all had the same z coordinate [actual range is 0.006 (1) or 0.04 (1) Å], then the space group would be *Cmcm*. Convergence in the latter group was rapid. The largest features in the final difference map have heights $\leq$ 0.13 and ≥ -0.12 e Å^{-3}.

Bond lengths and angles (Table 3) are normal except for C4—C9 and C3—C4—$C3^m$, which are affected by the inappropriate averaging, the disorder and the thermal motion. The atomic displacement ellipsoids are reasonable, if somewhat large (see Fig. 1). There is no elongation of the atomic ellipsoids in the direction perpendicular to the mirror plane such as would be expected if the mirror symmetry were approximate or if the *mmm* Laue symmetry were a consequence of twinning. The crystal packing is illustrated in Figs. 2 and 3.

The success of the RT pseudocell (or, substructure) refinement indicated that the amplitudes of the superstructure modulations must be small and that the superposition of the five independent half-molecules related by the pseudotranslation $b/5$ must give an electron-density distribution that is closer to being continuous than to being bimodal.

2.4.2. Room-temperature superstructure. The crystals look more monoclinic than orthorhombic because the ($hk\ell$) and ($h\bar{k}\ell$) directions are always so different (see §2.3), but none of the three cell angles are distinguishable from 90°. The agreement factor for averaging the data in Laue group 2/m is no better than for averaging in *mmm*. The C centering is unambiguous. The presence of a c glide is nearly certain; of the 37 $h0\ell$ and $h0\bar{\ell}$, ℓ odd, reflections measured with the KappaCCD diffractometer only two have $I > 3\sigma(I)$ [(001), I/σ = 13.0 and (20$\bar{5}$), I/σ = 4.5]. The only orthorhombic group consistent with the systematic absences is $Cmc2_1$.

The basic form of the superstructure modulation was worked out from the *CAD*-4 data using the program *PATSEE* (Egert & Sheldrick, 1985); the final model was worked out by trial and error. The modulation involves small rotations of the five independent half-molecules around the a axis;[3] the CMe_2 fragments in four of the five molecules are also disordered. The various possibilities for constraints and restraints available in *SHELXL*97 (Sheldrick, 1997) proved invaluable. We

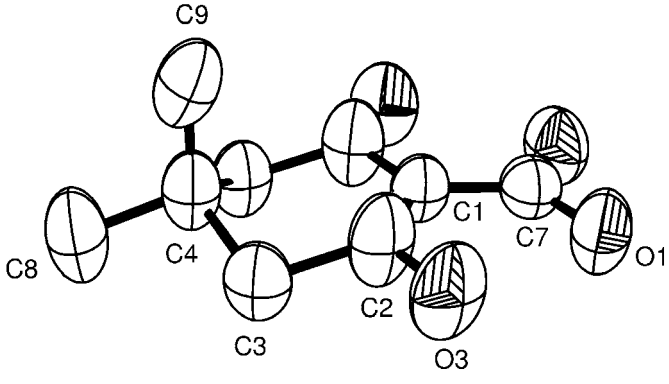

Figure 1
Perspective drawing of the molecular structure of ME2C7O4 at 295 K as determined in the pseudocell refinement of the n = 5 supercell. The shapes of the ellipsoids correspond to 50% probability contours of atomic displacement; H atoms have been omitted. The atom-numbering scheme is shown.

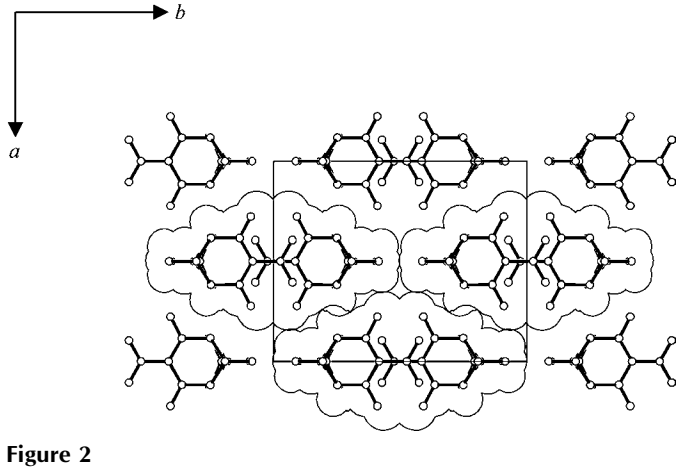

Figure 2
Projection of the pseudocell structure showing the molecular overlap. Cross sections of the van der Waals surfaces are shown for three molecular stacks.

[3] A rotation around **a** can also be described as a tilt with respect to **c** of the planar part of the molecule.

finally knew the structural model was satisfactory when the top five peaks in a difference Fourier map (0.19–0.22 e Å^{-3}) lay at the approximate midpoints of the five O1···O3 vectors, *i.e.* at the positions expected for the five missing H atoms. Refinement of the superstructure converged normally.

The presence of so much disorder in the final model worried us initially, but after the structure at 130 K had been solved and the structures of the two phases compared (see below), the extensive disorder made sense.

The basic atom-numbering scheme is the same for all molecules (see Fig. 1); the specific molecule is designated by a letter (*A*–*E*) at the end of the atom name. One of the five molecules (*C*) is completely ordered; each of the CMe_2 fragments in the other four molecules adopts two orientations. The occupancy factors for two of the major orientations [0.765 (5) for molecule *B* and 0.870 (6) for *E*] are substantially larger than are the occupancy factors for the other two major orientations [0.591 (5) for molecule *A* and 0.535 (4) for *D*].[4]

The final refinement cycles included many restraints. These included the condition that all chemically matched 1,2 and 1,3 distances be the same in the five molecules (instruction SAME 0.01 0.02) and a condition on the U^{ij} values within molecules (DELU 0.01 0.01) that is related to the Hirshfeld rigid-bond postulate (Hirshfeld, 1976; Rosenfield *et al.*, 1978). Atoms C4 and C4′ in molecules *B* and *E* were required to have the same coordinates (*EXYZ*), since the occupancy factors for the minor orientations were so low. The U^{ij} values for the atom pairs C3*n*/C3′*n* and C4*n*/C4′*n* were set to be equal (*EADP*) for all four disordered molecules (*n* = *A*, *B*, *D*, *E*). The minor positions of the methyl C atoms (C8′ and C9′) for molecules *B* and *E* were refined isotropically. The methylene and methyl H atoms were placed in calculated positions and then shifted with the attached C atom. The five hydroxyl H atoms were placed in the positions in which they appeared in the difference map and were constrained to ride on the neighboring O3 atom. A single U_{iso} value was varied for all five hydroxyl H atoms as a test. The final value [0.155 (8) Å^2] is large, presumably because each H atom can occupy two sites separated by *ca* 0.5 Å.

It is difficult to tell whether the molecular conformations of the five molecules of the RT structure differ. The angle between the planes composed of atoms O1, O3, C1, C2, C7 and their mirror images (eight atoms total) and the plane composed of atoms C3, C4 (or C3′ and C4′) and the mirror image of C3 (or C3′) is 38.0 (3)° at RT for the ordered molecule *C* and is 30.0 (6) and 33.4 (7)° for the two components of molecule *A*. The complete angular range is 26–40° (s.u.s ≤ 1°), where the three smallest values are for the minor components of molecules *B*, *D* and *E*.

An ellipsoid plot of the asymmetric unit is shown in Fig. 4. Bond lengths and angles (Table 3) are normal and vary little (because of the restraints) from one molecule to another. It was the combination of the reasonable agreement factors (Table 1), displacement ellipsoids and geometric parameters for this highly restrained refinement that convinced us that a good model for this exceptionally complicated structure had been found.

2.4.3. Low-temperature structure. Attempts in 1997 and at intervals thereafter to solve the low-temperature, *n* = 2 structure from the limited (θ_{max} = 16°) set of data were unsuccessful. It was only after we had finished refining the RT structure and had seen the likely analogy to the phase behavior of several cyclohexanediones (Katrusiak, 2000) that we found a structure solution. It might now be possible to collect a full set of data for the LT phase because measurements can be made so much more quickly with a CCD diffractometer, but there are no longer any crystals available. In any event the low-resolution structure is sufficient to answer the important questions; the details of the molecular geometry matter much less than does the overall packing arrangement.

The space group of the LT structure is not even approximately centered. There is almost certainly a *b* glide perpendicular to **c**; of the 69 *hk*0, *k* ≠ 2*n* reflections the two most

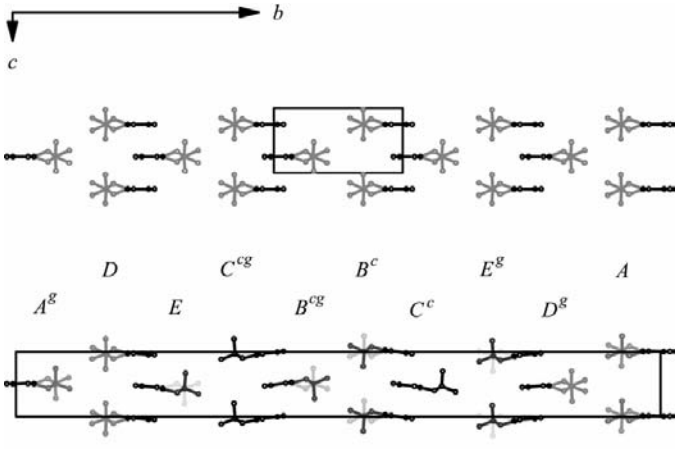

Figure 3
Projection of one {100} layer (centered at $x = \frac{1}{2}$) of the pseudocell structure (upper drawing) and of the full superstructure at room-temperature (lower drawing). Occupancy factors are coded by gray-scale shading. The designation C^{cg} indicates that molecule *C* has been taken through the glide and centering operations.

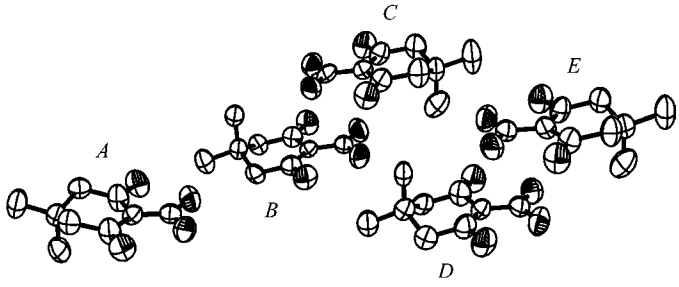

Figure 4
Perspective drawing of the asymmetric unit of the RT structure of ME2C7O4. The shapes of the ellipsoids correspond to 50% probability contours of atomic displacement; H atoms have been omitted. The atom-numbering scheme is the same as in Fig. 1; the designators for the molecules are shown.

[4] The values for the occupancy factors averaged over the five molecules are 0.63 and 0.37. These values can be compared to those found for the pseudocell refinement in *Cmc*21 (0.57 and 0.43).

intense have $I/\sigma_I = 2.5$ and 1.4. An *n* glide plane perpendicular to **b** is possible; of 17 $h0\ell$, $h + \ell \neq 2n$ reflections only the 001 reflection is present ($I/\sigma_I = 8.3$). The strong 103 reflection ($I/\sigma_I = 27$) seems to rule out the possibility of an *a* or *c* glide perpendicular to **b**. A 2_1 axis parallel **a** is likely; none of the three $h00$, $h \neq 2n$ reflections has $I/\sigma_I > 0.6$.[5]

We investigated packing arrangements and tried refinements in a number of primitive orthorhombic space groups; a successful model was eventually found in *Pmnb* (#62; an alternate setting of *Pnma*). The alternate setting was retained so that the axis labels could be the same as in the RT ($Cmc2_1$) structure. The asymmetric unit of the *Pmnb* structure contains two independent molecules that are related by a local twofold pseudorotation around **a** at $y = 0.3751\ (2) \simeq (3/8)$ and $z = 0.515\ (3) \simeq \frac{1}{2}$. Layers separated by **a**/2 are related by the approximate translation $0, \frac{1}{4}, 0$. There is a local *c* glide, as well as the true *n* glide, perpendicular to **b**.

The very low θ_{max} value and the location of so many atoms on mirror planes meant that the *Pmnb* refinement had to be highly constrained. In the end we decided to treat the two half-molecules as rigid groups and to refine nine U_{iso} values, *i.e.* one for each of the chemically different non-H atoms. The rigid groups (including H atoms) were based on the ordered molecule C of the full RT $Cmc2_1$ refinement. The various measures of the fit of the model (see Table 1) are satisfactory. The ratio N_{obs}/N_{var} is 482/20, but the restraints effectively reduce the number of variables even further (to 16; only one rigid-group rotation per molecule allowed to vary). The U_{iso} values (0.015–0.030 Å^2) show no unusual patterns; values are smallest for C1, C4 and C7, and largest for atoms C8, C9, O1 and O3. The peaks in the final difference map (see Table 1) are associated with atoms O3, C4, O1 and C1 and are located out of the molecular plane (see also below). We conclude that the basic features of the packing arrangement have been determined (see Fig. 5). It was possible to perform an acceptable, if restrained, anisotropic refinement ($R_1 = 0.062$, $wR_2 = 0.178$ for 79 parameters and 42 restraints), but the resulting ellipsoids, although not exceptionally eccentric, are neither pleasing nor informative. Allowing variation of the molecular conformations did not improve the fit.

It is possible that the true structure at 130 K is actually monoclinic, in which case the crystal we studied was a non-merohedral twin. The shattering of the crystal during data collection would be consistent with twinning, although the usual strains associated with cell contraction or chemical reaction are also a possible explanation.

[5] At the time the orientation matrix for data collection was determined we had no reason to think that the symmetry of the crystal might be lower than orthorhombic [$\alpha = 90.05\ (3)$, $\beta = 90.03\ (2)$, $\gamma = 89.96\ (3)^\circ$]. Two octants of data ($+h, +k, \pm\ell$) were collected, but unfortunately these do not allow testing for the equivalence of reflections that would be different ($+h, +k, +\ell$ and $-h, -k, \ell$) if **c** were the unique monoclinic axis. In any event the data do not average well ($R_{int} = 0.13$) even in $P11m$, perhaps partly because the reflections are generally weak ($R_{sig} = 0.11$).

3. Packing considerations

The crystal packing of ME2C7O4 is determined by the conflict between the packing preferences of the two regions of the molecule. The planar, polar, O-rich end (hereafter, the head) of the molecule and the tetrahedral, apolar, Me-rich end (hereafter, the tail) are so different electronically that intermolecular interactions between them should be minimized.[6] A packing arrangement in which the molecular heads and tails are segregated is expected.

Because the Me-rich tail of the molecule is about as thick as two of the O-rich heads, and because those heads are planar, the basic packing unit is a double stack of molecules (see Figs. 3 and 5) with methyl groups on the outside and the O-rich heads interleaved in the center. The observation that the **c** axis is the direction of fastest crystal growth supports the identification of the double stacks as the basic packing unit. Attractions within the stacks are stronger than attractions between stacks.

The cross section of a stack (see Fig. 2) is an approximate rhombus. The stacks are then rhombic prisms, which would be predicted to crystallize in the C-centered arrangement that is found for the subcell. The mirror planes relating the C═O and C—OH groups are retained in the crystal because the differences between the groups are too small to matter (see footnote **1**) and because the mirror is consistent with the C-centered packing.

The observation that two of the {110} faces of the pseudocell [*e.g.* (110) and $(\bar{1}\ \bar{1}0)$] are large while the other two are small or ill-formed indicates that crystal growth is relatively rapid in two of the pseudocell directions ⟨110⟩ (*e.g.* $[\bar{1}10]$ and $[1\bar{1}0]$), but slow in the other two. The crystal habit seemed at first to be inconsistent with the symmetry of the unit cell, but the habit can be understood if the contacts of the stack faces across (110) are generally favorable, but if the specific $CMe_2\cdots CMe_2$ contacts along **b** are not. Crystal faces {110} pass through all the unfavorable $CMe_2\cdots CMe_2$ contacts, but also separate interacting stacks. It seems likely that crystals nucleate from a small number of layers that include the directions [001] and (*e.g.*) $[\bar{1}10]$, along which growth is rapid; such a group of layers would include many interacting stacks, but relatively few $CMe_2\cdots CMe_2$ contacts. Growth perpendicular to those first layers would require the addition of layers (*e.g.* along [110], $[\bar{1}\bar{1}0]$, [010] or $[0\bar{1}0]$); such growth would be

[6] The segregation of electronically different parts of molecules into different regions of crystal structures is related to short-range order in solutions. The ΔH term for interactions of unlike molecules in solutions or unlike regions of molecules in crystals is influenced in part by the dispersion interactions, which are proportional to the products of the polarizabilities of the interacting units. If $P_A \neq P_B$, then $P_A^2 + P_B^2$ is greater than $2P_AP_B$ and ΔH will be positive for mixing. If stronger (*e.g.* dipolar) interactions are possible, the ΔH term for mixing is expected to be even more positive. Note that positive deviations from Raoult's Law are much more common than negative deviations; it is much more common for the activities of solution components to be greater than their mole fractions than less than their mole fractions. Most solutions form only because the $-T\Delta S_{mix}$ term is large enough to offset the positive ΔH_{mix} term. For ordered solid phases, in which $\Delta S_{mix} = 0$, segregation of different molecules into different crystals (*i.e.* fractional crystallization) or of different parts of a single molecule into different regions of a single crystal is the rule.

favored by interstack interactions, but hindered by $CMe_2\cdots CMe_2$ interactions. Crystal growth is therefore faster within an existing layer than perpendicular to it.

The $CMe_2\cdots CMe_2$ contacts cause crystal-packing problems because the length of **c** that would be optimal for space-filling by the Me groups is inappropriate for the overlap of the planar O-rich heads of the molecules. It must be that the spatial requirements of the O-rich heads are similar to those of an aromatic system, in which case the van der Waals thickness is approximately $2 \times 1.70 = 3.40$ Å (Pauling, 1960). The actual spacing in the RT structure (6.66 Å) is *ca* 2% shorter than $4 \times 1.70 = 6.80$ Å (see Fig. 3). That spacing, however, is longer than is needed for the Me groups on the outsides of the double stacks. The projection on **c** of the intramolecular vector between the two Me C atoms (C8 and C9) is 2.12 Å at RT in both the pseudocell refinement and in the ordered molecule *C* of the full refinement. Addition of 2×2.0 Å for the radii of the two methyl groups (Pauling, 1960) gives 6.12 Å for the thickness of the molecular tail, which is then *ca* 10% smaller than the space needed for two O-rich heads.

Space-filling representations of the *Cmcm* pseudocell structure show clearly that there is empty space between the axial Me groups of molecules in the same stack, even in the absence of any correlation between their orientations. These spaces would not, however, be large enough to allow significant interleaving of methyl groups of adjacent stacks, even if there were correlation. Contacts between equatorial Me groups in adjacent stacks are not very important either. Of the four possible arrangements of a $CMe_2\cdots CMe_2$ pair only one includes a short contact and that contact ($C8\cdots C8'$, 3.15 Å) is only about 0.05 Å shorter than expected. The Me groups just do not fit together very well; they are too far apart to fill space within the stacks and too close together to allow interleaving with the Me groups of an adjacent stack.

Tilting of the molecules in the stacks by $< 10^\circ$ has only a minor effect on the spacings within the stacks or the overall width of the stacks because $\cos 10^\circ = 0.985$. Tilting does, however, affect the relative energies of the two possible sites for the CMe_2 groups and may affect the molecular conformation if the less favorable site is occupied. The bond to the axial methyl group (C4—C9 vector) should point away from, or parallel to, the stack axis; the C4—C9 vector should never point into the stack.

The mismatch between thicknesses of the two ends of the molecule means that segregation of molecular heads and tails necessarily lowers the packing efficiency, but if the molecule were larger and more flexible it would probably be possible to find a better compromise.[7] Molecules of ME2C7O4 have only one low-energy intramolecular degree of freedom that affects the overall molecular shape (the out-of-plane displacement of the CMe_2 group) and significant differences in that coordinate are associated with relatively large changes in intramolecular energy.

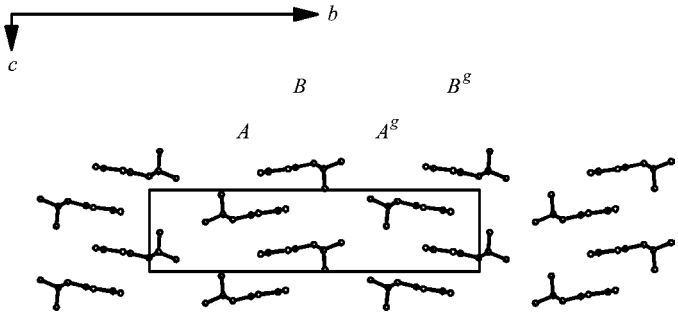

Figure 5
Projection of one {100} layer of the low-temperature structure. The mirror plane that passes through the molecules shown is at $x = \frac{1}{4}$. The designation A^g means that molecule *A* has been taken through the *b* glide operation.

4. Related structures

Only three structures containing the C(OH)C(COOH)C(═O) fragment were located in Version 5.21 (April 2001) of the Cambridge Structural Database (Allen & Kennard, 1993; hereafter the CSD). The simplest of these is 2-carboxy-3-hydroxyphenalenone (refcode KUXMAR; Sugawara *et al.*, 1992) in which a naphthyl fragment is fused to atoms numbered in ME2C7O4 as C3, C4 and $C3^m$. Since the thickness of this nearly planar molecule is about the same everywhere, the molecules form stacks within which neighboring molecules are related by pure translations. The perpendicular distance between molecules within stacks is 3.43 Å, which is a little longer than the spacing [$\frac{1}{2}$(6.66 Å) = 3.33 Å] found in ME2C7O4.

Molecules of 2-carboxy-1,3-benzo[*a*,*c*]tropolone (SUGCEC; Mochida *et al.*, 1992) also forms stacks by translation. The perpendicular distance between C(OH)C(COOH)C(═O) fragments, however, is longer (3.79 Å), presumably because of the 34° twist of the biphenyl fragment fused to the 'far' end of the seven-membered tropolone ring.

The third comparison compound is citrinin (CITNIN; Roversi *et al.*, 1996; Destro & Marsh, 1984; see also footnote **1**), which has a packing pattern similar to that of ME2C7O4. The stacking distance [$\frac{1}{2}$(7.291 Å) = 3.65 Å at RT] is longer than in ME2C7O4 because at the 'far' end of the molecule there are two axial Me groups rather than one. Space-filling drawings show that the Me groups are close packed, but that there are gaps between the O-rich heads of the molecules. Since the more loosely packed O-rich heads are rigid and cannot be disordered there is no phase transition between RT and 19 K (Roversi *et al.*, 1996).

The compound 2,6-dihydroxybenzoic acid (LEZJAB; see Davey *et al.*, 2001, and references therein) is closely related to

[7] Consider for example the structure of $F_3C(CF_2)_5(CH_2)_{11}OH$ (TULQOG; Lapasset *et al.*, 1996). The hydrogenated and fluorinated regions of the molecule are segregated in the crystal as expected. In order to achieve close packing the translational spacing for the hydrogenated region must be a little smaller than for the flourinated region. The spacing cannot differ unless the molecule is bent, so there is a 'kink' in the molecule produced by an unfavorable *gauche* interaction (C11—C12—C13—C14, 71°) around the first two fluorinated C atoms. As the two regions of the molecule are oriented differently with respect to the short (5.28 Å) stacking axis, the spacing between CF_2 groups is larger than the spacing between CH_2 groups.

ME2C7O4, but the extra hydroxyl proton means that there is intermolecular O—H···O bonding in both polymorphs.

5. The modulations

The RT and LT phases are both modulated variants of the *Cmcm* substructure. The important components of the modulations, and therefore of the transition between the two phases, are the rotations of the molecules around the cell axis **a** and the ordering of the CMe_2 fragments. In the *Cmcm* substructure, in which most atoms lie on a mirror plane perpendicular to **c** (see top of Fig. 3), the rotation angle is zero; the same mirror requires that the CMe_2 group be completely disordered. The pattern of rotations and occupancy factors in the full RT superstructure is complex, but the pattern of rotations in the LT phase becomes simpler and there is no disorder.

The molecular rotations are best measured by the angles made with the **c** axis of the eight-atom planes composed of atoms O1, O3, C1, C2, C7, $O1^m$, $O3^m$ and $C3^m$.[8] In the RT structure these angles are −0.7, −7.7, −8.0, −3.7 and −5.9° (all s.u.s ≤ 0.05°) for molecules *A*–*E* (see Fig. 3). The value, which is always < 90°, is positive if a clockwise rotation would bring the normal to the eight-atom plane into coincidence with **c** or **−c.** At 130 K the corresponding angles are 9.2 and 8.2° (s.u.s 0.1°) for molecules *A* and *B*. The difference in sign of the rotations in the two phases is a consequence of the choice of coordinate system.

The structure is composed of molecular stacks that interact poorly along **b** (see §3). In the RT structure a layer at $x = \frac{1}{2}$ (see Fig. 3) is composed of stacks made up of molecules *A* and A^g ($\langle y\rangle = 0$), of *D* and *E* ($\langle y\rangle \simeq 1/5$), of C^{cg} and B^{cg} ($\langle y\rangle \simeq 2/5$) and of their *c*-glide related partners. The average values for the molecular rotations within these stacks are then $\frac{1}{2}(0.7 - 0.7) = 0.0°$ for $A + A^g$, $\frac{1}{2}(-3.7 - 5.7) = -4.7°$ for $D + E$, and $\frac{1}{2}(8.0 + 7.7) = +7.8°$ for $C^{cg} + B^{cg}$. The full set of rotation (or tilt) angles for the stacks at $x = \frac{1}{2}$ and with $0 \le y \le 1$ is then 0.0, −4.7, +7.8, −7.8, +4.7 and 0.0 (the glide operation changes the sign). These values fit well (r.m.s. deviation = 0.1°) to the equation $(-8.2°)\sin(4\pi y)$, where *y*, the coordinate of the stack axis, is 0, 1/5, 2/5 *etc*. This equation can also be written as $(-8.2°)\sin(4\pi n/5)$, where *n*, the stack number, is 0, 1, 2, 3, 4, 5 = 0 *etc.*

In the LT phase (see Fig. 5) the repeat along **b** is composed of two, rather than five, stacks and the two stacks are related by the *b* glide. The average rotation angles for the stacks are therefore $\pm\frac{1}{2}(9.2 + 8.2) = \pm 8.7°$. The equation for the modulation wave is $(8.7°)\cos(2\pi n/2)$, where *n* is 1, 2, 3 = 1 *etc.* The two wavevectors are then $2\mathbf{b}'^*/5 = 0.4\mathbf{b}'^*$ for the RT structure (two cycles in five subcells) and $\mathbf{b}'^*/2 = 0.5\ \mathbf{b}'^*$ for the LT structure (one cycle in two subcells), where $\mathbf{b}'^*$ is the reciprocal axis of the subcell. The amplitudes of the modulation waves in the two phases are comparable.

The description of the waves as functions of the position along **b** of the stack center supports the identification of the $CMe_2\cdots CMe_2$ interactions as the origin of the modulations.

Another way to view the RT structure is as a sort of hybrid of the *Cmcm* pseudocell structure (stack $A + A^g$) and of the LT phase (stacks $C^{cg} + B^{cg}$ and $B^c + C^c$; see Fig. 3); the latter set of stacks, along with molecules *E* and E^g, can be superimposed nearly exactly on the LT structure. Stack $D + E$ (rotation angles −3.7 and −5.7°), or perhaps just the half-stack *D*, forms the transition region between the tilted and untilted stacks. This structural pattern explains the intensity statistics for the $k = 5n \pm m$ reflections; stacks separated by $\Delta y = 2/5$ differ more than stacks separated by $\Delta y = 1/5$ so the reflections having $k = 5n \pm 2$ are much stronger than those having $k = 5n \pm 1$.

The $k = 5n \pm 2$ reflections are the first-order superstructure reflections, because the modulation wave is $2\mathbf{b}'^*/5$ and the $k = 5n \pm 1$ reflections are the second-order reflections. The greater intensity of the first-order superstructure reflections is consistent with the sine function described above being the most important component of the modulation wave; the presence of the second-order reflections indicates that the sine function is not the only component of the wave.

The modulation waves also explain the occupancy factors; in general, the larger the tilt angle, the greater the deviation of the methyl-group occupancy factors from $\frac{1}{2}$. The occupancy factors, however, are also influenced by the disorder of molecules adjacent within the layer. The factors for the methyl groups of molecule *A* [$\frac{1}{2} \pm 0.09$ (1)] are nearly equal because the planar part of the molecule is nearly parallel to **c**. The factors for molecule *D* [$\frac{1}{2} \pm 0.04$ (1)] are nearly the same because the methyl groups of molecule *D* are interleaved with those of molecule *A*. The occupancy factors of molecule *E* [$\frac{1}{2} \pm 0.37$ (1)] differ more than would be predicted from the molecular rotation angle because the methyl groups of *E* interleave with those of molecule *C*, which has the largest rotation angle and is completely ordered. The methyl groups of molecule *B* are more disordered than might be expected [occupancy factors $\frac{1}{2} \pm 0.26$ (1)], perhaps because the effects of interlayer interactions have been ignored. Stacks of *B* molecules are separated by $\pm\mathbf{a}/2$ from columns of the fully disordered *A* molecules.[9]

[8] In the RT structure the mirror operation is $-x, y, z$ for molecules *B* and *C* and $1 - x, y, z$ for molecules *A*, *D* and *E*. In the LT structure the mirror operation is $\frac{1}{2} - x, y, z$ for both molecules.

[9] The spacing along **b** of the midpoints of stacks composed of molecules $A + A_g$ ($\langle y\rangle = 0$) and molecules $D + E$ ($\langle y\rangle \simeq 1/5$) might be expected to be a little larger than the spacing of the midpoints of stacks composed of molecules $C^{cg} + B^{cg}$ ($\langle y\rangle \simeq 2/5$) and $B^c + C^c$ ($\langle y\rangle \simeq 3/5$). The actual spacings are $b/5 + 0.009$ (3) and $b/5$–0.020 (3) Å. The shifts have the expected sign, but are small in magnitude, probably because the C-centering of the RT cell puts $A + A^g$ stacks immediately in front of and behind the region between of the $C^{cg} + B^{cg}$ stacks and $B^c + C^c$ stacks. The *C*-centering means that any expansion or contraction along **b** associated with the differences in molecular tilts and distributions of the Me groups can be local only. No differences in overlap of the O-rich, planar regions of the molecules in the three independent ($A + A^g$, $B + C$ and $D + E$) stacks can be seen.

6. Comparison of the RT and LT phases

The differences between the $Cmc2_1$ and *Pmnb* phases (and the *Cmcm* substructure) are consequences of the way the Me groups interact. In the $A^g + D$ regions of the RT structure (and in the substructure) there is little correlation of CMe_2 orientations and little interleaving of the Me groups. In the LT phase the CMe_2 groups are ordered and **b** is 1.0% shorter; these changes suggest a closer fit of the Me groups in adjacent stacks.

The packing coefficient (Spek, 2001), which is low for both structures, increases from 0.65 to 0.67 between 295 and 130 K. In this temperature range the length of **a** is effectively constant. The change in **c** is largest (−3.4%); the interplanar distance between the O-rich heads decreases by *ca* 0.13 Å.[10]

7. Discussion

Observation of a high-symmetry disordered structure at a higher temperature and a lower-symmetry ordered structure at a lower temperature is not uncommon for molecular crystals (see *e.g.* Katrusiak, 2000). Crystals of ME2C7O4 are noteworthy because the RT form is a complex, modulated superstructure rather than a completely disordered structure with $Z' \leq 1$, and because the unit cell of the LT structure is smaller and has a higher symmetry than the unit cell of the RT structure. The RT phase is also unusual because of the large number of molecules in the asymmetric unit; large values of Z' are more common for crystals that have been studied at temperatures below the temperature of crystal growth.[11]

The *Cmcm* substructure is so important in the RT structure, and so significant to the LT structure, that we suspect it is the structure of the critical nuclei. It is difficult to imagine that the 66 Å axis of the RT structure could be established during the very first stage of crystal growth when the crystals are composed of a countable number of molecules.[12] The crystal morphology and habit suggest (see §3) that growth in directions that require the incorporation of $CMe_2\cdots CMe_2$ contacts is slow. While the crystallites are still very small the orientations of adjacent CMe_2 groups must be completely uncorrelated; only after the crystals become larger can the long-range modulation lock in.

The reason for the C centering in the superstructure is unclear. That operation requires that modulation waves in layers {100} separated by **a**/2 be out of phase.

The differences in the TS terms for the different structures hint at the energy differences between phases. In the proposed *Cmcm* nucleus the $kT\ln\omega^n$ contribution to the free energy is $RT\ln 2 = 1.70$ kJ mol^{-1} at 295 K if the orientations of the CMe_2 groups are completely random. In the partially ordered $Cmc2_1$ structure the $kT\ln\omega^n = -(RT/5)\Sigma(x_i \ln x_i)$ contribution at 295 K is 1.13 kJ mol^{-1} if the orientations are random and less if they are not. As the temperature is lowered the $kT\ln\omega^n$ contribution to the free energy becomes less important both because T becomes smaller and because order almost certainly increases.[13] At some temperature above 130 K the gain in energy associated with the denser *Pmnb* structure is greater than the loss of the free energy associated with the disorder and a transition to the ordered phase occurs. The TS terms suggest that this energy difference cannot be much greater than 1 kJ mol^{-1}.

Throughout the phase sequence the molecular stacks have at least approximate 2/*m* symmetry (twofold axis parallel to **a**). In the *Cmcm* substructure that symmetry is exact, in the $Cmc2_1$ superstructure it is approximate and in the *Pmnb* structure it is nearly exact. Exact 2/*m* symmetry in the *Pmnb* phase is impossible because it is incompatible with the requirement that layers {100} separated by **a**/2 be offset along **b** by half the interstack distance. The approximate 2_1 screw axis that relates the CMe_2 tails within a layer is a local operation for the same reason.[14]

8. Summary

Molecules of ME2C7O4 have trouble packing because they are small and rigid, are composed of two regions that are very different electronically, and are about, but not quite, twice as thick at one end as at the other. The molecules form stacks that are approximate rhombic prisms; the prisms interact well along their sides but poorly at their pointed ends. The result of these packing problems is a modulated, significantly disordered superstructure at RT with five independent, mirror-symmetric molecules [$Z' = 5 \times (\frac{1}{2}) = 2.5$].

Crystals of ME2C7O4 undergo a transition to an ordered phase between RT and 130 K. Both phases can be described as modulated variants of a completely disordered *Cmcm* substructure; the two phases differ in the tilts of the molecules relative to the stacking axis **c** and in the ordering of the CMe_2

[10] At 130 K the interplanar distance is $\frac{1}{2}$(6.434 Å)cos 8.7° = 3.18 Å. At 295 K that distance is $\frac{1}{2}$(6.662 Å)cos α, where α is the average tilt angle of the stack; the distances are 3.33, 3.32 and 3.30 Å for α = 0.0, 4.7 and 7.8°.

[11] Modulated structures are more often encountered when crystals grown at one temperature are studied at a lower temperature. In many of those crystals there is an intermolecular interaction that is acceptable when the vibrational amplitudes are larger, but which becomes impossible as the vibrational amplitudes decrease; the classic example is biphenyl (Baudour, 1991, and references therein; see also Busing, 1983). The RT structure of ME2C7O4, however, does not fit in this class because crystals were studied at the same temperature at which they were grown and because there are no 'short' intermolecular contacts in the *Cmcm* pseudocell structure. The packing problem that leads to the modulation appears to be too much, rather than too little, space per molecule. Even in the LT structure the methyl groups are not in good contact along **c**.

[12] The number of molecules in a crystal nucleus of critical size is uncertain, but has been estimated to be 'typically a few tens of molecules' (Bernstein *et al.*, 1999).

[13] Since there is no symmetry relationship between the two orientations of each of the four disordered molecules the depths of the energy wells should differ and the occupancy of the deeper of each pair of wells should increase as the temperature is lowered.

[14] Individual stacks should have symmetry 2/*m*. Stacks adjacent along **b** (see Fig. 5) should be related by 2_1 screw axes parallel to **c** so that the Me-rich tails of the molecules can be interleaved; this requirement suggests the distance between the two stacks should be *b*/2. Stacks adjacent along **a** should be displaced along **b** by $\frac{1}{2}(b/2) = b/4$ so that the substructure is C-centered (see Fig. 2). There is no space group that allows all these requirements to be met exactly.

groups. The complicated RT phase can also be understood as a hybrid of a fully disordered phase and of the phase seen at LT.

The structure was solved, refined and interpreted using standard small-molecule techniques, but the effort required was substantial. Such complicated structures are almost certainly less rare in nature than they are in the CSD.[15]

We are indebted to Professor Martin Stiles, who synthesized this interesting compound and then resynthesized it for us several times over a period of many years, and to the Referees and Co-Editor, who helped us with the description of the modulations. We are also pleased to acknowledge the help of Professors J. D. Dunitz (ETH, Zurich) and A. L. Spek (Utrecht), with whom we have had many discussions about phase transitions and high-Z' structures.

References

Allen, F. H. & Kennard, O. (1993). *Chem. Des. Autom. News*, **8**, 1, 31–37.
Altomare, A., Cascarano, G., Giacovazzo, C., Guagliardi, A., Burla, M. C., Polidori, G. & Camalli, M. (1994). *J. Appl. Cryst.* **27**, 435–436.
Baudour, J. L. (1991). *Acta Cryst.* B**47**, 935–949.
Bernstein, J., Davey, R. J. & Henck, J.-O. (1999). *Angew. Chem. Int. Ed. Engl.* **38**, 3441–3461.

[15] Complicated sequences of phases are better known (see *e.g.* van Smaalen, 1995) for substances that would be archived in the inorganic or metals databases than for substances that would be archived in the CSD, perhaps because crystals in the former group are likely to scatter more strongly and are more likely to be studied using X-ray film methods, powder diffraction and/or electron microscopy/diffraction than are molecular crystals. The greater energies associated with long-range interactions in non-molecular crystals may also increase the probability of the occurrence of modulated structures.

Brock, C. P. & Dunitz, J. D. (1994). *Chem. Mater.* **6**, 1118–1127.
Busing, W. R. (1983). *Acta Cryst.* A**39**, 340–347.
Davey, R. J., Blagden, N., Righini, S., Alison, H., Quayle, M. J. & Fuller, S. (2001). *Cryst. Growth Des.* **1**, 59–65.
Destro, R. & Marsh, R. E. (1984). *J. Am. Chem. Soc.* **106**, 7269–7271.
Egert, E. & Sheldrick, G. M. (1985). *Acta Cryst.* A**41**, 262–268.
Enraf–Nonius (1988). *CAD*-4 *User's Manual*, Version 5.0. Enraf–Nonius, Delft, The Netherlands.
Hirshfeld, F. L. (1976). *Acta Cryst.* A**32**, 239–244.
Katrusiak, A. (1992). *J. Mol. Struct.* **269**, 329–354.
Katrusiak, A. (2000). *Acta Cryst.* B**56**, 872–881.
Lapasset, J., Moret, J., Melas, M., Collet, A., Viguier, M. & Blancou, H. (1996). *Z. Kristallogr.* **211**, 945–946.
Mochida, T., Shinagawa, H., Izuoka, A. & Sugawara, T. (1992). *Chem. Lett.* pp. 1623–1626.
Nonius (1998). *COLLECT*. Nonius BV, Delft, The Netherlands.
Nonius (1999). *COLLECT*. Nonius BV, Delft, The Netherlands.
Otwinowski, Z. & Minor, W. (1997). *Methods Enzymol.* **276**, 307–326.
Pauling, L. (1960). *The Nature of the Chemical Bond.* Ithaca, New York: Cornell University Press.
Rosenfield, R. E., Trueblood, K. N. & Dunitz, J. D. (1978). *Acta Cryst.* A**34**, 828–829.
Roversi, P., Barzaghi, M., Merati, F. & Destro, R. (1996). *Can. J. Chem.* **74**, 1145–1161.
Sheldrick, G. M. (1990). *SHELXTL/PC.* Siemens Analytical Instruments Inc., Madison, Wisconsin, USA.
Sheldrick, G. M. (1997). *SHELXL*97. University of Göttingen, Germany.
Smaalen, S. van (1995). *Crystallogr. Rev.* **4**, 79–202.
Spek, A. L. (2001). *PLATON*. Utrecht University, The Netherlands.
Sugawara, T., Mochida, T., Miyazaki, A., Izuoka, A., Sato, N., Sugawara, Y., Deguchi, K., Moritomo, Y. & Tokura, Y. (1992). *Solid State Commun.* **83**, 665–668.
Xia, A., Selegue, J. P., Carrillo, A., Patrick, B. O., Parkin, S. & Brock, C. P. (2001). *Acta Cryst.* B**57**, 507–516.